Confocal Scanning Laser Microscopy Studies of Crystal Growth During Oxidation of a Liquid FeO-CaO-SiO_2 Slag

ANNA SEMYKINA, JINICHIRO NAKANO, SEETHARAMAN SRIDHAR, VOLODYMYR SHATOKHA, and SESHADRI SEETHARAMAN

The oxidation of FeO in 30 wt pct FeO-35 wt pct CaO-35 wt pct SiO_2 slag was investigated as part of a wider study on the recovery of Fe units through magnetic separation. A confocal scanning laser microscopy (CSLM) technique was used to visualize the oxidation of FeO in the liquid slag. The formation event was observed *in situ* under the CSLM and the onset of precipitation on a surface of the slag liquid was recorded at various temperatures in an oxidizing atmosphere. A Time-Temperature-Transformation (TTT) diagram was constructed based on the CSLM results. Samples obtained from the CSLM heating chamber were analyzed by a scanning electron microscope (SEM) equipped with an energy-dispersive spectrometer (EDS).

DOI: 10.1007/s11663-011-9505-6

I. INTRODUCTION

THROUGH the production of iron and steel, large amounts of industrial wastes and by-products are generated. Efficient recycling of these materials is of increasing interest worldwide as a result of increasing sustainability in processes with respect to increasing raw material costs and waste reduction.

For example, for the Swedish and Ukrainian steel industry, the steelmaking slag contains up to 30 wt pct wustite (FeO). It is important to maximize the amount of iron that is recovered from this slag so that the remaining portion can be used for civil engineering purposes. To find a practical solution, joint efforts are currently underway at the Royal Institute of Technology, Sweden; National Metallurgical Academy of Ukraine; and Carnegie Mellon University.

A sustainable approach to use steelmaking slag components based on the transformation of nonmagnetic iron monoxide (or wustite) to magnetite by oxidation has been proposed by the current authors.[1] This allows the selective recovery of iron-bearing and non–iron-bearing slag constituents for specific purposes. From the technological point of view, pretreated slag is processed using a magnetic method wherein iron oxides transformed to a magnetic form are separated for subsequent use. The rest of the slag (nonmagnetic) could be used effectively in the production of cement binder or in other applications. Magnetic products may be used as a component for sintering mixture or for pelletizing iron ores.

The phase equilibria in the slags containing iron oxides have been reported by several authors, including Turkdogan,[2] Bodsworth and Bell,[3] and Muan and Osborn.[4] Pownceby *et al.*[5] focused on the phase equilibria of Fe_2O_3-CaO-SiO_2 in air at 1513 K to 1573 K (1240 °C to 1300 °C) with the effects of basicity on the phases indicated. Lin-nan Zhang *et al.*[6] analyzed the oxidation mechanism in CaO-FeO_x-SiO_2 slag with high iron content, using pure oxygen.

In our previous work,[7] the kinetics of oxidation of the FeO-CaO-SiO_2 system in air at the temperature range of 1623 K to 1773 K (1350 °C to 1500 °C) was investigated by Termogravimetric technique application. The current work investigates the mechanism of oxidation of Fe^{2+} to Fe^{3+} in molten slags by using a confocal scanning laser microscopy (CSLM) technique at the temperature range of 1530 K to 1600 K (1257 °C to 1327 °C). The slags investigated were synthetic and of the 30 wt pct FeO-35 wt pct CaO-35 wt pct SiO_2 system.

II. EXPERIMENTAL

A. *Materials and Sample Preparation*

CaO powder with a purity of 99.9 pct and SiO_2 powder with a purity of 99.5 pct were supplied by Sigma Aldrich Chemie (Munich, Germany). SiO_2 and CaO powders were dried prior to weighing. FeO (wustite) was synthesized and examined by X-ray diffraction (XRD). The details of the synthesis were described in the previous work.[8] Platinum crucibles for holding the slags were 99.99 pct in purity and had dimensions of 5 mm in diameter × 5 mm in height × 0.4 mm in thickness. Argon and air were supplied by Valley

ANNA SEMYKINA, Senior Researcher, is with the Division of Materials Process Science, Royal Institute of Technology, SE-10044 Stockholm, Sweden, and with the National Metallurgical Academy of Ukraine, Dnipropetrovsk 49600, Ukraine. Contact e-mail: annase@kth.se JINICHIRO NAKANO is with the Department of Materials Science and Engineering, Carnegie Mellon University, Pittsburgh, PA 15213 and is Principal Research Scientist with National Energy Technology Laboratory, 1450 Queen Ave., Albany, OR 97321. SEETHARAMAN SRIDHAR, POSCO Professor, is with the Department of Materials Science and Engineering, Carnegie Mellon University. VOLODYMYR SHATOKHA, Professor and Vice Rector, is with the National Metallurgical Academy of Ukraine. SESHADRI SEETHARAMAN, Professor, is with the Division of Materials Process Science, Royal Institute of Technology.

Manuscript submitted July 13, 2010.
Article published online March 29, 2011.

National Gas (Pittsburgh, PA). Alumina crucible-supports (8 mm in diameter × 5 mm in height × 0.5 mm in thickness) for confocal microscopic studies were supplied by ULVAC (Kanagawa, Japan).

B. *Apparatus and Procedure*

1. *Confocal scanning laser microscope*

In the current study, the crystal formation event was measured optically *in situ* through a CSLM (Lasertec 1LM21H, Yokohama, Japan), and the onset of observable precipitation on the surface of the liquid slag was imaged and recorded at various temperatures in air. The experimental assembly has been described in detail in the previous publication.[8] It should be noted that at the beginning of the oxide formation, the gas oxygen potential had likely not reached its desired value and the slag would not be equilibrated with the atmosphere. The experiments were performed above the liquidus temperature of the slag. According to the Slag Atlas (2nd ed.),[9] the liquidus temperature of studied slag composition should be ≈1500 K (1227 °C).

In the experimental setup used, a cylindrical platinum crucible containing approximately 0.030-g slag was placed on a high-density alumina crucible. The whole sample was then set on a platinum sampler pan (10 mm diameter). In the beginning of experiment, the CSLM chamber was evacuated for 10 minutes and was purged with argon gas for 20 minutes at a rate of 200 mL/min. Each slag sample in the Pt-crucible was then heated at the CSLM hot stage in an Ar (purity 99.999 pct) atmosphere. To start from a completely molten slag, the sample was heated initially to 1700 K (1427 °C) and maintained for 20 minutes until it melted completely. The sample was then slowly (5 °C/min) cooled down to the desired aim temperature. The atmosphere in the heating chamber was then switched from Ar to air so that the designated oxygen partial pressure was obtained for magnetite/hematite precipitation. Before the experiments, the temperature calibration for the crucible holder was performed. The temperature of the samples was controlled by a proportional–integral–derivative (PID) controller unit and adjusted continuously to compensate for a heat change during oxidation reactions occurring over the atmospheric switch from Ar to air with a flow rate of 200 mL/min.

A temperature calibration for the sample holder was carried out using a two-thermocouple technique. The first thermocouple was attached directly to the sample holder while the second one was introduced close to the bottom of the platinum crucible. The reading from the latter was assumed to be the actual temperature, whereas the sample holder thermocouple was the set temperature. The sample (actual) temperature showed a negative deviation compared with the holder temperature.[8]

III. RESULTS

A. *CSLM Studies*

To study the formation event of crystals during the initial oxidation reaction, imaging through a CSLM technique was carried out. The precipitation behavior of the oxide particles during oxidation will be discussed first.

The crystal growth observed by the CSLM is presented in Figure 1. In the beginning of the experiment, the powder sample (Figure 1(a)) was heated to 1700 K (1427 °C) until it became completely molten in the argon atmosphere.

After melting, the sample was cooled slowly to the desired temperature and the argon gas was switched to air,

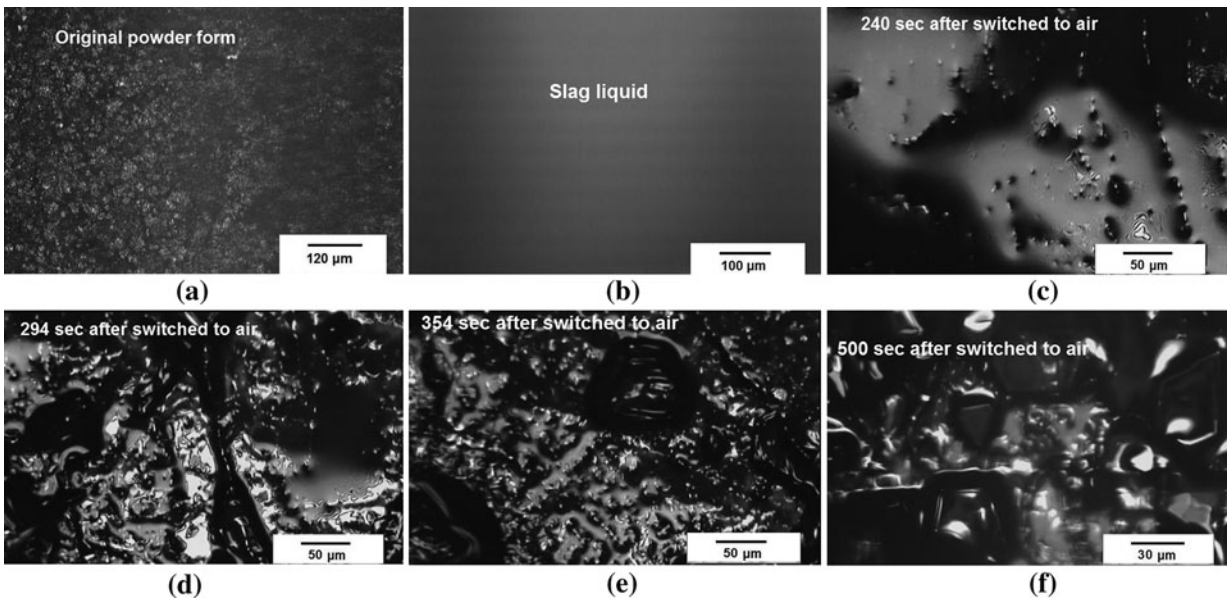

Fig. 1—Crystals observed by the CSLM for sample at 1593 K (1320 °C) (oxidation in air): (*a*) sample as original powder form at room temperature; (*b*) molten sample; (*c*) crystal formation after switching to air; (*d*)–(*f*) crystal growth and agglomeration with time.

while the temperature was maintained constant (Figure 1(b)). The time until the air reached the sample surface for the current gas flow rate was found to be approximately 40 seconds. This time was estimated based on the time when the temperature started to change because of the oxidation reactions after the gas switch. The first crystals were observed after 240 seconds of air introduction (Figure 1(c)). With time, the crystals grew (Figure 1(d)) and agglomerated (Figures 1(e) and (f)). The observed crystal size in the beginning was ≤4 μm. With time, crystals grew and agglomerated with their sizes reaching 40 to 50 μm in some cases.

The time until observable crystal precipitation took place was measured through *in situ* visualization using the CSLM and recorded at various temperatures. The crystal lengths was measured with time. A corresponding Time-Temperature-Transformation (TTT) diagram with average data was then constructed as shown in Figure 2, where two curves were identified. A node of the lower curve seems to be located slightly above 1530 K (1257 °C) where the fastest kinetics was found, whereas that of the upper curve seems to be located around 1570 K (1297 °C). As temperature was raised, slopes of these curves rapidly decreased, indicating that the crystals required more time to form.

The crystals obtained at different temperatures corresponding to the TTT diagram are presented in Figure 3.

For the temperature range of 1570 K to 1600 K (1297 °C to 1327 °C), crystals 20–40 μm in length were observed (Figure 3(a)) with geometry different from those obtained at lower temperatures. At 1560 K (1287 °C), observed crystals were relatively dispersed and somewhat angular (Figure 3(b)). At the temperature range of 1550 K to 1530 K (1277 °C to 1257 °C), crystals were smaller (<5 μm in some cases) and rather clustered (Figure 3(c)). These observations imply that nucleation occurred at a faster rate at 1533 K (1260 °C), where nucleation sites were saturated quickly, whereas crystals precipitated at 1593 K (1320 °C) could grow larger. This corresponds well with the TTT diagram shown in Figure 2. The TTT diagram shows a break in the temperature range of 1560 K to 1570 K (1287 °C to 1297 °C). A possible cause of this discontinuity (*i.e.*, the presence of two distinct curves) is a change in the precipitating phase. To study this phenomenon, three samples at three different temperatures were quenched in the CSLM chamber in Ar atmosphere at the maximum cooling rate with 74 °C/s from 1580 K to 1073 K (1307 °C to 800°C) and analyzed using a scanning electron microscopy (SEM)-energy-dispersive spectrometer (EDS).

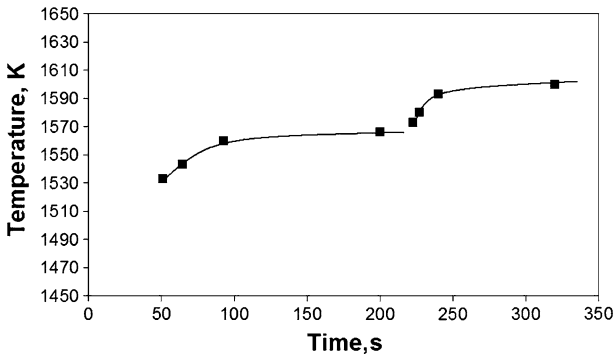

Fig. 2—TTT diagram for the 30 wt pct FeO-35 wt pct CaO-35 wt pct SiO_2 system.

B. *SEM-EDS Results*

Quenched samples from the CSLM chamber were analyzed by SEM-EDS. SEM images of the quenched samples are presented in Figure 4. The resultant EDS analyses were summarized in Table I. The EDS analysis has been done on the single spot marked as (1) in Figure 4.

According to Table I, the iron content in the spot marked (1) in Figure 4(c) is lower than that in Figure 4(b). Because of the SEM spatial resolution limit, the analyzed area in Figure 4(c) might be covering both iron oxide and calcium silicates.

IV. DISCUSSION

A. *Thermodynamic Aspect*

FeO in molten slags can be oxidized to magnetite or hematite, and if they are exposed to an environment oxidizing enough to raise the oxidation degree of Fe. The following reactions may take place:

$$3(FeO)_{slag}+1/2O_2 = (Fe_3O_4)_{solid} \quad [1]$$

$$2(FeO)_{slag}+1/2O_2 = (Fe_2O_3)_{solid} \quad [2]$$

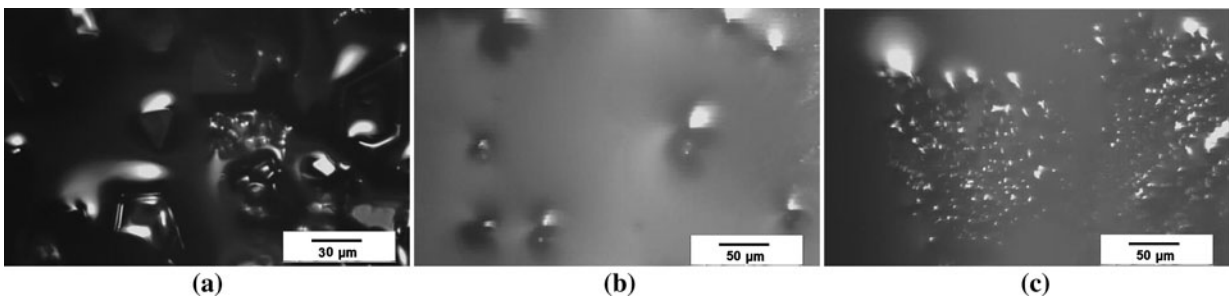

Fig. 3—The CSLM images for samples treated in air at (*a*) 1593 K (1320 °C), (*b*) 1560 K (1287 °C), and (*c*) 1533 K (1260 °C).

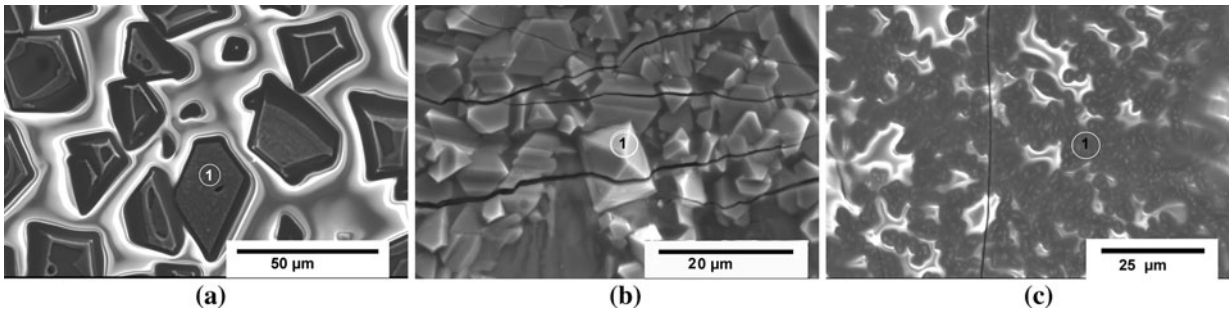

Fig. 4—SEM images for the samples quenched from: (*a*) 1580 K (1307 °C); (*b*) 1560 K (1287 °C); (*c*) 1533 K (1260 °C).

Table I. EDS Results of the Quenched Samples (Marked (1) in the figures) from the CSLM Chamber, Corresponding to Fig. 4

Element	Atomic Pct
Figure 4(a) (1)	
O	58.80
Si	18.99
Ca	20.19
Fe	2.02
Total	100.00
Figure 4(b) (1)	
O	60.3
Si	10.87
Ca	10.81
Fe	18.02
Total	100.00
Figure 4(c) (1)	
O	58.74
Si	15.785
Ca	16.785
Fe	8.69
Total	100.00

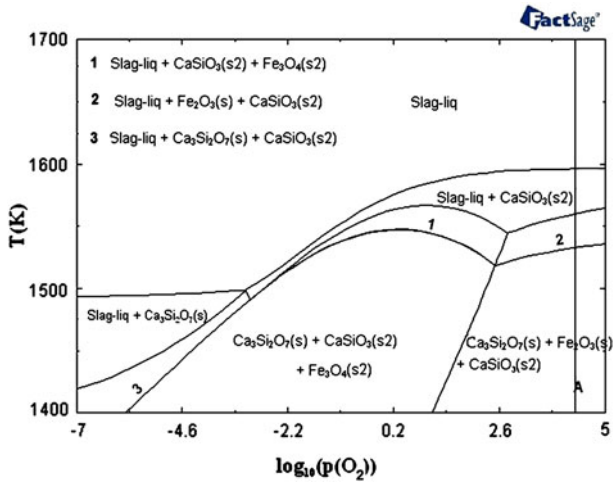

Fig. 5—Temperature *vs* partial pressure of oxygen phase diagram. The line marked **A** corresponds to the partial pressure of oxygen in air. P_{O_2} is presented in Pa. Calculated using FactSage 6.1.

To find out what phases can be obtained in the current oxidation atmosphere, a thermodynamic calculation was performed by using FactSage 6.1 (Thermfact Ltd., Montreal, Canada and GTT Technologies, Aachen, Germany). Figure 5 represents a phase diagram, temperature *vs* partial pressure of oxygen in the system.

As the experiment was conducted above 1500 K (1227 °C), the initial atmosphere was argon. The experimental conditions were confirmed to be located in the fully liquid region of the Figure 5. After switching to air, the FeO was oxidized, and depending on the temperature, crystals precipitated in accordance with the need to attain thermodynamic equilibrium as depicted in Figure 5.

In air over a temperature range of 1560 K to 1600 K (1287 °C to 1327 °C), calcium silicate ($CaSiO_3$) can be obtained in the liquid slag (Figure 5), which might correspond to the crystals with different morphology (Figure 3(a) and 4(a)).

According to the phase diagram, hematite and calcium silicate can form in the liquid slag over a temperature range of 1530 K to 1560 K (1257 °C to 1287 °C) when exposed to air. The CSLM investigation at 1560 K (1287 °C) shows commonly found morphology of the crystals (somewhat cubic shape; Figures 3(b) and 4(b)). EDS analyses of the quenched sample indicated the presence of calcium silicate and iron oxide. At a temperature of 1533 K (1260 °C) (which corresponds to the border between two regions: solid $Ca_3Si_2O_7$, hematite, $CaSiO_3$ and liquid slag containing hematite and $CaSiO_3$), similar types of crystals were found by CSLM.

The TTT diagram shows a discontinuity in the temperature range of 1560 K to 1570 K (1287 °C to 1287 °C), which corresponds to conditions expected to cause the hematite formation when this slag is exposed to air per Figure 5. The EDS analysis of the sample quenched from 1560 K (1287 °C) showed higher concentration of iron oxide in precipitated crystals than those observed in the sample obtained at 1580 K (1307 °C). The sample quenched from 1580 K (1307 °C) mainly contained calcium silicate ($CaSiO_3$).

From Figure 5, it can be also observed that over a range of $\log_{10}(P_{O_2}) = -3.0$ through 2.0, FeO in slag may be oxidized to magnetite [<1560 K (1287 °C)]. To produce magnetite, it is advantageous to use a lower partial pressure of oxygen rather than air (*e.g.*, CO_2 gas, CO/CO_2 mixture or Ar).

The data obtained in the present study and previous experience of the authors allowed offering the following

strategies aimed at maximizing the yield of iron in the form of magnetite:

(a) To perform oxidizing at lower temperatures with subsequent quenching in inert atmosphere as soon as first precipitates appear.
(b) To control a partial pressure of oxygen with *e.g.*, additives of CO_2 in order to tailor precipitation within the area where Fe_3O_4 is present among the solid products. Our previous studies[10] have demonstrated this possibility.
(c) Simultaneous processing of steelmaking and *e.g.*, ferromanganese slag. It was found by the current authors that with manganese oxide in the synthetic slag system, magnetite can be obtained as a spinel as well as manganese ferrite.[8] Manganese in the slag stabilizes the magnetite and arrests subsequent oxidation to hematite, as it was found for the ternary system.

B. *Kinetic Analyses of the Crystal Growth*

The oxidation process can be controlled by the following steps:

(a) Nucleation of magnetite/hematite during the initial oxidation reaction
(b) Chemical reaction
(c) Oxidation due to diffusion of oxygen/iron through the product layer

Once a crystal is nucleated, three possible ways for crystals to grow on the slag surface can be considered. First, the gas/solid interface can grow into the gas phase when iron cations diffuse across the crystal phase to the interface where they react with oxygen. Second, when oxygen anions diffuse across the crystal phase to the liquid/solid interface, this interface moves into slag by interacting with iron cations. In the third scenario, the triple point where gas, liquid, and solid meet can laterally grow without solid-state diffusion involved. The growth can occur when the sufficient amount of iron cations and oxygen anions interact at the interface.

Provided that dissociation rates are comparable in all the three cases, growth at the triple point may occur most easily because of (1) larger interfacial energy and (2) faster diffusion in the gas phase (gas-phase mass transfer) and in the liquid phase (liquid-phase mass transfer). The three possible rate controlling steps for this growth are as follows:

(a) Gas-phase mass transfer control: If it is assumed that Fe^{z+} is always sufficiently available at the interface, diffusion of O_2 through the diffusion boundary layer controls the reaction rate.
(b) Liquid-phase mass transfer control: If Fe^{z+} requires long range diffusion and its supply is slow, the gas flow rate and gas-phase mass transfer rate have a negligible effect on growth of crystals compared with the diffusivity of Fe^{z+}.
(c) Mixed control of mechanisms 1 and 2.

From the obtained CSLM images, the length of the crystals was measured with time. The average data were plotted In Figure 6.

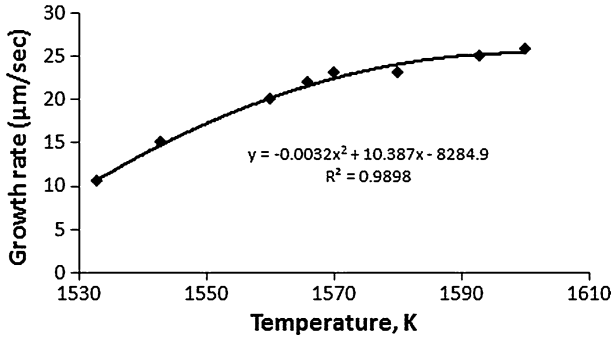

Fig. 6—The measured growth rates of the crystals in air at different temperatures (average data).

The growth rate of crystals increased with temperature. Similar behavior was found during the studies of quaternary FeO-MnO-CaO-SiO_2 system.[8] This could be indicative of a faster rate of transport in the liquid phase as a result of a lower viscosity.

The current TTT diagram for the crystal formation at the gas/liquid slag interface (Figure 2) showed that, with an increase in temperature, the start of the precipitation is delayed as well. This could be caused by lower degree of super saturation for crystal precipitation as the temperature is increased.

V. CONCLUSIONS

In the current work, the kinetic study of oxidation of FeO in the liquid slag has been conducted by CSLM. The real-time confocal analysis showed the crystal formation behaviors during oxidation of FeO in a 30 wt pct FeO-35 wt pct CaO-35 wt pct SiO_2 liquid slag. With time, the crystals grew and agglomerated, reaching, in some cases, 40 μm in length. Different shapes of crystals were observed at different temperatures. At temperatures >1560 K (1287 °C), the crystals reached 20–40 μm in length. According to the thermodynamic calculations, this type of crystal corresponds to the calcium silicate phase. In the temperature range of 1530 K to 1560 K (1257 °C to 1287 °C), crystals had somewhat a cubic shape and corresponded to the expected formation of hematite (Fe_2O_3). A TTT diagram was constructed based on the CSLM results.

ACKNOWLEDGMENTS

The authors are thankful to Swedish Foundation for Strategic Environmental Research (MISTRA) for the financial support through the project Eco-Steel Production (Sub project no.: 88035) administered by Swedish Steel Producers Association (Jernkontoret). The financial support for Anna Semykina from the Swedish Institute is gratefully acknowledged.

REFERENCES

1. A. Semykina, V. Shatokha, and S. Seetharaman: *Molten 2009*, Santiago, Chile, 2009, p. 65.
2. E.T. Turkdogan: *Fundamentals of Steelmaking*, The Institute of Materials, Cambridge, UK, 1996, pp. 156–57.
3. C. Bodsworth and H.B. Bell: *Physical Chemistry of Iron and Steel Manufacture*, Longman, London, UK, 1972, pp. 343–45.
4. A. Muan and E.F. Osborn: *Phase Equilibria Among Oxides in Steelmaking*, Addison-Wesley, Reading, MA, 1965, pp. 33, 86.
5. M.I. Pownceby, J.M.F. Clout, and M.J. Fisher-White: *Trans. Inst. Min. Metall.*, 1998, vol. 107, pp. C1–C10.
6. L.-N. Zhang, L. Zhang, M.-Y. Wang, and Z.-T. Sui: *Transactions of the Nonferrous Metals Society of China*, Nonferrous Metals Society of China, 2005, vol. 15, pp. 938–43.
7. A. Semykina, V. Shatokha, M. Iwase, and S. Seetharaman: *Metall. Mater. Trans. B.*, 2010, vol. 41B, pp. 1230–39.
8. A. Semykina, J. Nakano, S. Sridhar, V. Shatokha, and S. Seetharaman: *Metall. Mater. Trans. B*, 2010, vol. 41B, pp. 940–45.
9. Verein Deutscher Eisenhuttenleute, ed.: *Slag Atlas*, 2nd ed., Verlag Stahleisen GmbH, Dusseldorf, Germany, 1995.
10. A. Semykina, V. Shatokha, and S. Seetharaman: *Ironmaking Steelmaking*, 2010, vol. 37 (7), pp. 536–40.